NAVAL POSTGRADUATE SCHOOL
Monterey, California

THESIS

OBJECTIVE ANALYSIS OF A COASTAL OCEAN EDDY USING SATELLITE AVHRR AND IN SITU HYDROGRAPHIC DATA

by

Rogério Paulo Antunes Chumbinho

September 1993

Thesis Advisor: Roland W. Garwood, Jr.
Co-Advisor: Robert L. Haney

Approved for public release; distribution is unlimited.

DISCLAIMER NOTICE

THIS DOCUMENT IS BEST QUALITY AVAILABLE. THE COPY FURNISHED TO DTIC CONTAINED A SIGNIFICANT NUMBER OF COLOR PAGES WHICH DO NOT REPRODUCE LEGIBLY ON BLACK AND WHITE MICROFICHE.

REPORT DOCUMENTATION PAGE

1a. REPORT SECURITY CLASSIFICATION: UNCLASSIFIED	1b. RESTRICTIVE MARKINGS
2a. SECURITY CLASSIFICATION AUTHORITY	3. DISTRIBUTION/AVAILABILITY OF REPORT: Approved for public release; distribution is unlimited
2b. DECLASSIFICATION/DOWNGRADING SCHEDULE	
4. PERFORMING ORGANIZATION REPORT NUMBER(S)	5. MONITORING ORGANIZATION REPORT NUMBER(S)
6a. NAME OF PERFORMING ORGANIZATION: Department of Oceanography, Naval Postgraduate School; 6b. OFFICE SYMBOL (if applicable): 35	7a. NAME OF MONITORING ORGANIZATION: Naval Postgraduate School
6c. ADDRESS (City, State, and ZIP Code): Monterey, CA 93943-5000	7b. ADDRESS (City, State, and ZIP Code): Monterey, CA 93943-5000
8a. NAME OF FUNDING/SPONSORING ORGANIZATION; 8b. OFFICE SYMBOL (if applicable)	9. PROCUREMENT INSTRUMENT IDENTIFICATION NUMBER
8c. ADDRESS (City, State, and ZIP Code)	10. SOURCE OF FUNDING NUMBERS: PROGRAM ELEMENT NO. / PROJECT NO. / TASK NO. / WORK UNIT ACCESSION NO.

11. TITLE (Include Security Classification)
OBJECTIVE ANALYSIS OF A COASTAL OCEAN EDDY USING SATELLITE AVHRR AND IN SITU HYDROGRAPHIC DATA

12. PERSONAL AUTHOR(S)
Rogério Paulo Antunes Chumbinho

13a. TYPE OF REPORT	13b. TIME COVERED	14. DATE OF REPORT (Year, Month, Day)	15. PAGE COUNT
Master's Thesis	FROM TO	1993, September, 23	51

16. SUPPLEMENTARY NOTATION
The views expressed in this thesis are those of the author and do not reflect the official policy or position of the Department of Defense or the United States Government.

17. COSATI CODES		
FIELD	GROUP	SUB-GROUP

18. SUBJECT TERMS (Continue on reverse if necessary and identify by block number)
Hydrographic and Satellite Data, Correction of Satellite Data, Data Visualization, Objective Analysis, Multiquadric Interpolation.

19. ABSTRACT (Continue on reverse if necessary and identify by block number)

A common characteristic of the interaction between the coastal topography and eastern boundary currents (EBC) is the appearance of cold filaments and mesoscale eddies. Hydrographic and satellite temperature data obtained during a cruise on board R/V Point Sur off Point Arena, California, in May 1993 were analyzed to study a particular eddy field in this area.

The hydrographic data was first used to verify the remotely sensed surface temperature field, using three dimensional data visualization. Selected vertical levels from each hydrographic station were then interpolated into a broader, finer resolution grid domain in preparation for an eventual model initialization, using multiquadric interpolation.

The results verify the existence of the eddy and show its signature in the vertical to about 300 meters depth. A sensitivity study of interpolation parameters was performed to evaluate approximately the optimal set of parameters, showing that the multiquadric interpolation resolves very well the temperature field in the upper levels and introduces small amplitude, small scale noise in the deeper levels. This noise can be eliminated by a more thorough parameter sensitivity study.

20. DISTRIBUTION/AVAILABILITY OF ABSTRACT: [X] UNCLASSIFIED/UNLIMITED [ ] SAME AS RPT. [ ] DTIC USERS	21. ABSTRACT SECURITY CLASSIFICATION: UNCLASSIFIED
22a. NAME OF RESPONSIBLE INDIVIDUAL: Roland W. Garwood, Jr.	22b. TELEPHONE (Include Area Code): (408) 656-3260; 22c. OFFICE SYMBOL: OC/Gd

DD FORM 1473, 84 MAR — 83 APR edition may be used until exhausted. All other editions are obsolete.

19. Continued:

A comparative analysis of satellite AVHRR data, in situ hydrographic data and interpolation results shows that the eddy did not experience significant horizontal translation during the period of the cruise suggesting that the asynopticity between the different data sets is not significant for the purpose of objectively analyzing the temperature field.

Approved for public release; distribution is unlimited

OBJECTIVE ANALYSIS OF A COASTAL OCEAN EDDY USING SATELLITE AVHRR AND IN SITU HYDROGRAPHIC DATA

by
Rogério Paulo Antunes Chumbinho
Lieutenant, Portuguese Navy
B.S., Portuguese Naval Academy, 1986

Submitted in partial fulfillment of the
requirements for the degree of

MASTER OF SCIENCE IN PHYSICAL OCEANOGRAPHY

from the

NAVAL POSTGRADUATE SCHOOL
September 1993

Author: Rogério P. Antunes Chumbinho
Rogério Paulo Antunes Chumbinho

Approved By:

Roland W. Garwood, Jr., Thesis Advisor

Robert L. Haney, Thesis Co-Advisor

Curtis A. Collins, Chairman,
Department of Oceanography

ABSTRACT

A common characteristic of the interaction between the coastal topography and eastern boundary currents (EBC) is the appearance of cold filaments and mesoscale eddies. Hydrographic and satellite temperature data obtained during a cruise on board R/V Point Sur off Point Arena, California, in May 1993 were analyzed to study a particular eddy field in this area.

The hydrographic data was first used to verify the remotely sensed surface temperature field, using three dimensional data visualization. Selected vertical levels from each hydrographic station were then interpolated into a broader, finer resolution grid domain in preparation for an eventual model initialization, using multiquadric interpolation.

The results verify the existence of an eddy and show its signature in the vertical to about 300 meters depth. A sensitivity study of interpolation parameters was performed to evaluate approximately the optimal set of parameters, showing that the multiquadric interpolation resolves very well the temperature field in the upper levels and introduces small amplitude, small scale noise in the deeper levels. This noise can be eliminated by a more thorough parameter sensitivity study.

A comparative analysis of satellite AVHRR data, in situ hydrographic data and interpolation results shows that the eddy did not experience significant horizontal translation during the period of the cruise suggesting that the asynopticity between the different data sets is not significant for the purpose of objectively analyzing the temperature field.

TABLE OF CONTENTS

LIST OF TABLES

LIST OF FIGURES

ACKNOWLEDGMENT

I wish to express my appreciation to Dr. Steven Ramp, for making the hydrographic data available for this study, as well as to Dr. Wendell Nuss for providing the code for the three dimensional multiquadric interpolation.

I. INTRODUCTION

Following the early interest in the strong and well developed western boundary currents such as the Gulf Stream and the Kuroshio, the oceanographic community is becoming aware of the importance of the eastern boundary currents in the dynamics of the ocean. This is particularly true in the coastal zone, where the interaction between the eastern boundary currents and the boundary is strongest.

Eastern boundary currents (EBC) are typically characterized as a slow, broad and shallow equatorward flow with diffuse boundaries or transition zones separating them from the local coastal currents. Gill (1982) summarizes several aspects of EBC, including driving mechanisms, non-local influences due to coastally trapped waves, bottom friction and topography effects, upwelling, frontogenesis and turbulence. An intricate circulation results from this complex system where cold filaments extending offshore and permanent and recurring eddies are common features.

Eddy activity in EBC regions has been observed as early as the mid nineteen sixties, but the general perspective of the extent of eddy phenomena in time and space was only made possible by the more recent availability of satellite observations (Pares-Sierra *et al.*, 1993). Since then, eddies and filaments have been observed in eastern ocean boundaries using different types of remotely sensed and/or in situ observations (e.g., Pares-Sierra *et al.*, 1993; Sousa, 1992; Strub *et al.*, 1991; Ramp *et al.*, 1991; Haynes *et al.*, 1991).

A useful technique for the study of eddies and cold filaments is numerical simulation (e.g. Pares-Sierra *et al.*, 1993; Batteen *et al.*, 1992). Numerical models require some form of observed or statistical data for initialization, forcing and verification. Although satellites are becoming an important source of regular and nearly synoptic observations, oceanographic data is in general sparse, and spatial and temporal gaps are common, presenting difficulties in model initialization or data assimilation.

Several methods to interpolate and optimize observed fields for use in models have been developed (see Haltiner and Williams,1980, for a good description of the interpolation and initialization methods commonly used in numerical modeling). These methods use data correlation and/or historical data to relate observations collected in an irregular observational space to information projected into a regular model grid. The transformation must be able to keep the interpolated fields within realistic bounds and be able to preserve the state of slight imbalance between the mass and motion fields that ultimately drives the system. The purpose of this study is to objectively grid and analyze a coastal ocean eddy seen in satellite Advanced Very High Resolution Radiometer (AVHRR) and in situ hydrographic data, making use of the fairly recent multiquadric interpolation method (Hardy, 1971; Nuss, 1993) to interpolate and prepare observed fields in two and three dimensions. Multiquadric interpolation is the chosen method because it has proven superior qualities over other methods (e.g., Barnes and Cressman objective analyses) in the objective analysis of the observed fields and reduction of spurious high wavenumber noise in space (Nuss and Titley, 1993).

Data collected from 21 to 25 May 1993 by R/V Point Sur off Point Arena, California, is processed with the ultimate objective of being used to initialize a coastal ocean circulation model. We begin by describing the data and its collection methods in the next section, followed by data analysis, multiquadric interpolation description, and results. The final section includes conclusions and suggestions for future work.

II. DATA COLLECTION

A. SATELLITE DATA

The satellite data used in this work consists of images obtained from the Oregon State University. The images were from channel four of the Advanced Very High Resolution Radiometer (AVHRR) flying on the National Oceanic and Atmospheric Administration (NOAA) series of Earth observing satellites. This sensor observes the surface of the Earth in the infrared region (IR) with wavelengths between 10.5 and 11.5 μm. The temperature data were computed by converting radiometer counts to temperatures directly without any correction for water vapor (atmospheric correction), because no other channels were available to perform a multispectral correction.

After downloading the images from Oregon State University via Internet, further processing was done at the Naval Postgraduate School using software developed at the University of Florida, Miami. This processing consisted of correcting the images for appropriate navigation (geographical correction) and remapping the entire image into the region of interest, centered at a point off Point Arena, California. The ground resolution depends on the distance between each particular pixel and the satellite nadir and is in the range of 1 to 3 km. A suitable colormap was then applied to enhance the range of temperatures of the ocean surface and make more visible the regions contaminated by clouds. A mask was applied over land.

The satellite derived temperatures were obtained by forcing a linear relationship between pixel value and temperature value. To obtain the satellite temperature series (SAT) in Figure 2, for example, the image for day 22 May 1993 was sampled at the same positions of the CTD stations, and the pixel value was read and divided by ten to convert to temperature, thus providing a resolution of one tenth of a degree Celsius.

Most of the images collected during the period of the cruise contained large amounts of cloud cover; for this reason, only the images for days 21 and 22 May (23 Greenwich Mean Time) were used in this work (see Figures 3 and 4).

B. HYDROGRAPHIC DATA

The hydrographic data used in this study was collected during a Naval Postgraduate School cruise on board R/V Point Sur, between the 21st and the 25th of May, 1993, using a Neil Brown Mark III Conductivity, Temperature and Depth (CTD) instrument. The CTD casts were performed on an array of stations listed in Table 1 (see also Figure 1).

TABLE 1: CHARACTERISTICS OF THE CTD STATIONS

LONG (W)	*LAT (N)*	*NUMBER*	*DATE*	*TIME (h)*	*MAX Z (m)*
-123.697	38.546	1	22	23.9	500
-123.779	38.643	2	22	22.7	460
-123.857	38.750	3	22	21.4	410
-123.951	38.859	4	22	20.0	455
-124.027	38.970	5	22	18.5	530
-124.176	38.889	6	23	10.6	2420
-124.080	38.782	7	23	8.3	2110
-123.984	38.675	8	23	6.0	1965
-123.917	38.587	9	23	4.0	1940
-123.811	38.478	10	23	1.8	1630
-123.940	38.393	11	23	24.0	2280
-124.026	38.493	12	23	21.2	3125
-124.100	38.591	13	23	18.8	2500
-124.212	38.700	14	23	16.1	3200
-124.313	38.808	15	23	12.8	3260
-124.456	38.703	16	24	11.4	3500

TABLE 1: CHARACTERISTICS OF THE CTD STATIONS

LONG (W)	*LAT (N)*	*NUMBER*	*DATE*	*TIME (h)*	*MAX Z (m)*
-124.332	38.595	17	24	9.1	3445
-124.239	38.507	18	24	6.4	3430
-124.131	38.414	19	24	4.2	3430
-124.027	38.318	20	24	2.0	3430
-124.149	38.236	21	25	11.6	3600
-124.248	38.338	22	25	9.4	3670
-124.356	38.422	23	25	0.6	3650
-124.467	38.525	24	24	22.0	3605
-124.574	38.621	25	24	19.6	3660
-124.787	38.807	26	24	14.5	3610
-124.681	38.714	27	24	16.9	3650
-124.498	38.356	28	25	3.8	3760
-124.629	38.282	29	25	6.0	3840
-124.049	38.150	30	25	13.6	3610
-123.948	38.061	31	25	15.7	3510
-123.842	37.966	32	25	17.9	3480

The instrument's pressure, temperature and conductivity sensors were calibrated prior and after the cruise. A General Oceanics rosette sampler was used to collect in situ water samples for conductivity calibration after the cruise. The CTD sampling rate was 32 Hz. The raw data was collected and processed using a software package developed at EG&G Marine Instruments. The processing done at this level consisted of removing bad data points (outliers) using a first difference criteria to detect suspicious data points and linear interpolation to perform the correction. The data was then averaged to every 2 dbar and recorded in files for posterior data analysis.

An underway data acquisition loop was active during the cruise, automatically recording averages of temperature and salinity data at the 2 m depth (among other data) every 30 seconds (Ship's Data Acquisition System). This surface data was used in this study to fill data void areas and will be hereafter referred to as SAIL data (see section III.B.2).

Moored current meters (Acoustic Doppler Current Profiler - ADCP - and conventional rotor meters) were also deployed at station numbers 3, 7, 8, 9, 13, 17, 18, 19 and 23. The ADCP is able to measure the three components of the current using an array of four acoustic beams; the Doppler shift induced in the returning echoes by the moving column of water is processed to compute the absolute three dimensional current vector. An appropriate time gating of the echo yields a profile of the velocity field in the vertical between the instrument and the bottom for downward looking ADCP sensors, or between the instrument and the surface for upward looking sensors, at several depth bins (for more details on the ADCP instrument, see Acoustic Doppler Current Profilers, 1989).

The ADCP sensors deployed in this cruise were looking upward from the top of the mooring, providing current measurements from 300 m depth to the surface. In addition to the moored ADCP instruments, a hull mounted ADCP looking downward recorded velocity data continuously following the track of the ship. An example of the final product combining the moored and hull mounted ADCP data is presented in Figure 5. This figure shows the horizontal current vectors corresponding to the depth bin 15-23 m with velocities in cm s^{-1}. This current meter data was used in the analysis of the surface temperature field.

III. DATA ANALYSIS

A. SATELLITE DATA

Since the satellite data consisted only of radiances measured by channel four of the AVHRR, the analysis of the satellite data collected during the cruise period presents two major problems: the comparison of the remotely sensed sea surface temperatures (SST) with in situ observations in order to determine the amount of atmospheric influence on the sensed image and the correction of the satellite data for atmospheric influences in order to make the data usable in later stages of the work.

Figure 2 illustrates the method used to determine the corrections to be applied. The CTD series was obtained by averaging the first five meters of temperature readings at each station and ordering the results by time of CTD cast. The satellite series was obtained by sampling the image in Figure 4 at the positions of the CTD stations. These two spatial series contain a time lag introduced by the lack of synopticity of the CTD data; the time of the satellite image is comparable to the time of the first few CTD stations. The difference between the two series is thus not only due to atmospheric effects (which are not time dependent) but also due to a time-varying term (see Figure 2, middle plot). This latter term contains information on the movement of the eddy shown in Figure 4 that can be estimated by carefully comparing the CTD data collected in the final part of the cruise with the satellite data from two or three days earlier. This information on the motion of the eddy during the period of the hydrographic cruise can be useful for adjusting the analysis for asynopticity, and to evaluate the performance of a prediction model started from the analysis.

The problem of making the satellite observations usable can then be regarded in two ways: either making the CTD stations "more synoptic" relative to the satellite data or adjusting the satellite data to the weakly synoptic CTD data that we know is the "truth" in

its time/space frame, correcting the atmospheric term in the process. Both approaches remove the trend in the temperature difference in the middle frame of Figure 2, in a least squares sense, and shift the satellite series over the in situ series. This adjustment was accomplished by fitting least squares straight lines to both series, computing the point-by-point difference between these two lines and finally adding the point-by-point difference to the original satellite series. The bottom plot in Figure 2 shows that the results obtained are very satisfactory. A comparison of the variability of the corrected satellite series relative to the CTD series and the variability of the CTD series itself is given by the ratio:

$$\frac{\langle [T_{CTD} - T_{SAT}]^2 \rangle}{\langle [T_{CTD} - \langle T_{CTD} \rangle]^2 \rangle} \qquad \text{(III.1)}$$

where T_{CTD} is the CTD temperature series, and T_{SAT} is the series of adjusted satellite-derived temperatures taken at the positions of the CTD stations. The angled brackets represent ensemble averages. For the data shown in the bottom frame of Figure 2 this ratio is 0.44. The mean square difference between the adjusted satellite series and the CTD series is thus smaller than the variance of the CTD series, meaning that the values of the adjusted satellite series may be regarded as representative of the sea surface temperature.

This procedure guaranties the best possible match between the two series at each CTD station position and also inside a domain defined by the outer stations through bilinear interpolation of the correction terms. For positions outside this domain, the satellite readings may be corrected using averages of the nearest-neighbor correction terms.

The purpose of these corrections is to be able to use satellite-derived sea surface temperatures with a minimum atmospheric effect in the multiquadric interpolation *outside* the area defined by the CTD stations, since it is desired to analyze a region somewhat larger than that defined by the CTD array (see Figures 4 and 9). The satellite-derived temperatures will influence the surface values for the areas not covered by CTD stations in the horizontal, and this will augment the data for interpolating in the vertical for the underlying column of

water. It will be shown later that this influence is significant in the final surface temperature maps produced by the multiquadric interpolation.

B. HYDROGRAPHIC DATA

1. Analysis of CTD Stations

The data collected in the CTD casts as described in the previous chapter were first analyzed to determine to what extent the features visible in Figure 4 were not an atmospheric phenomenon, such as local wind swirls induced by coastal topography. For this purpose a visualization software package available from Silicon Graphics, Inc. was used (Explorer, 1993).

The CTD stations provide both temperature and salinity data over a range of depths. For simplification in the visualization, only the stations lying within a more or less regular square were used. This includes stations 1 through 25. The maximum depth considered was 2001 m; station numbers 1 through 5 and 8 through 10 do not reach this depth due to the shoaling bottom. Although bottom topography will be included in future work, a similarity method was used here to extend the profiles below the shallow parts of the bottom topography down to the 2001 m depth, in order to achieve a regular three dimensional domain. This method searches for temperatures in the nearest profile equal to the deepest temperature in the profile to be extended. After the match is found, the lower part of the nearest profile is copied to the profile to be extended. The similarity method is attributed to Helland-Hansen, but no citation was found. The method reflects the theory that a horizontal temperature (or any other conservative property) line in a particular region can be found in the vertical in some position away from this region due to the general oceanic circulation (slow sinking and spreading).

The vertical resolution of the raw CTD data is one data point every 2 m, starting at z=-1 m. To reduce computer memory requirements, the profiles were sampled at 52 preselected levels (every 2 m from -1 to -11, every 4 m from -11 to -19, every 6 m from -19 to -43, 8 m to -51, every 10 m from -51 to -101, every 20 m from -101 to -301, every

30 m from -301 to -481, 40 m to -521, every 50 m from -521 to -671, 60 m to -731, 70 m to -801 and every 100 m from -801 to -2001).

The data were visualized by Explorer using a perimeter coordinate system, with uniform grid spacing in the horizontal (approximately 14 km) and arbitrary spacing in the vertical, to allow selection of different levels and the setting of an appropriate aspect ratio for visualization. Some images resulting from the CTD visualization are shown in Figures 6 through 8. Of particular interest is Figure 8 showing a map of the surface temperatures as measured by the CTD. Since only 25 CTD stations were used in the visualization, the locations of the grid points are clearly evident due to the coarse resolution. However, a comparison of this map with Figure 4 shows that the main concentrations of cool and warm water were also defined by the CTD casts, thus verifying that Figure 4 does indeed represent an oceanic eddy. At the same time, Figure 7 shows a fluctuation of the main thermocline that corresponds well to the warm and cold waters at the surface, demonstrating the vertical manifestation of the eddy. The eddy appears to have a definite signature in the upper 300 m, in agreement with other sources of data including current meter data. Further discussion on the correspondence between the raw CTD data, the satellite images and the results of the interpolation scheme will be presented in Chapter IV.

The vertical structure of the data is in fact quite complex. Isothermal surfaces are often found folded several times, particularly in the upper levels, perhaps due to observational errors. However, it is expected that the vertical motions in a coastal eddy like the one considered here may be large, and these could lead to vertical distributions of temperature and salinity that would allow folding of isotherms and still maintain the hydrostatic stability of the water column. Static stability analysis was not carried out in the present raw data analysis, but it will be considered in future work. Both temperature and salinity data are available for the computation of the three dimensional density field that can be visualized in the same way the temperature field is, providing a quick way to determine the stability of the entire water column defined by the CTD stations.

In order to improve the visual appearance of the raw CTD data, and to prepare it for input into an ocean prediction model with approximately 2 km resolution, the CTD observations must be interpolated onto such a grid. The method of multiquadric interpolation used for this purpose is described in the next section.

2. Multiquadric Interpolation

We begin with a description of the method, following closely that provided by Nuss (1993). Consider a three dimensional irregular surface containing a field sampled at N observation points. For each observation point we know the location (x,y,z) and the value of the field (H). This irregular surface can represent almost any scalar field; for this work, H is temperature.

The interpolation of the field value in any arbitrary point X is based on a weighted sum of radial basis functions:

$$H(X) = \sum_{i=1}^{N} \alpha_i Q(X - X_i), \qquad \text{(III.2)}$$

where α_i is the weight of the *kernel* function Q, its argument being the radial distance between the point X and the observation point X_i. For multiquadric interpolation, the kernel function is a hyperboloid function:

$$Q(X - X_i) = [(X - X_i)^2 + c^2]^{1/2}. \qquad \text{(III.3)}$$

The constant c is an arbitrary small number to keep the function from vanishing at the observation points. For three dimensional interpolation, the kernel function is therefore:

$$Q(X - X_i) = [(x - x_i)^2 + (y - y_i)^2 + (z - z_i)^2 + c^2]^{1/2}. \qquad \text{(III.4)}$$

To solve for the weights, we apply Equation III.2 to all N observation points, resulting in a set of N equations with N unknowns:

$$H(X_j) = \sum_{i=1}^{N} \alpha_i Q_i(x_j, y_j, z_j) \quad . \tag{III.5}$$

In matrix notation, the solution is given by:

$$\alpha_i = Q_{ij}^{-1} \cdot H_j, \tag{III.6}$$

where Q_{ij} is a square matrix of equation coefficients. This matrix was inverted using Matlab's matrix inversion function (Matlab, 1992), in the two dimensional case, and using routines available in the LINPACK library of mathematical routines (Linpack, 1978), in the three dimensional case.

Once the weights are known, the interpolated solution to any point (e.g., regularly spaced grid points) is then given in matrix notation by:

$$H_g = Q_{gi} \cdot \alpha_i, \tag{III.7}$$

where:

$$Q_{gi} = [(x_g - x_i)^2 + (y_g - y_i)^2 + (z_g - z_i)^2 + c^2]^{1/2}, \tag{III.8}$$

(x_g, y_g, z_g) being the coordinates of each regular grid point. The two dimensional problem is just a particular case of the more general three dimensional case, with all z coordinates set to zero. The matrix on the left hand side has as many rows as there are grid points, but the number of columns is always equal to the number of observation points. In other words, the solution depends only on the number of observation points available and is independent of the size of the grid to be interpolated.

The method presented above is valid for noise-free observations. Unfortunately, real data include observational errors that must be taken into account. This is achieved through the introduction of an uncertainty parameter and a smoothing parameter (Nuss and Titley, 1993) in Equation III.5. In matrix notation:

$$H_j = [Q_{ij} + N\lambda\sigma_i^2 \cdot \delta_{ij}] \cdot \alpha_i, \tag{III.9}$$

where λ is the smoothing parameter, σ_j^2 is a vector of uncertainties in the observations (mean-squared observation error) and δ_{ij} is the Kronecker delta function. The difference now is that the diagonal elements of Q_{ij} are modified to include a factor involving those two parameters. Note that the uncertainties vector can have different values for different observation points, an useful property that gives the user of the method enough freedom to optimally set the parameters for best fitting any part of the grid.

There are several judgements that must be made when this method is to be used. The first two are selecting the values of the smoothing parameter λ and the interpolation constant c. The smoothing parameter determines how damped the interpolated field will be, and its value will depend on the application and kind of data being interpolated; large values imply strongly damped analyses. The interpolation constant has also some smoothing associated with it, but its major effect is on the shape of the basis functions. Large values imply rather flat interpolating functions and thus tight gradients or closely spaced observation points are not well represented. The values for these parameters depend to a large extent on the particular application. While research is still going on to determine optimum values for c and λ, setting them remains a trial and error process.

Another factor to be considered is the aspect ratio of the vertical to the horizontal scales. In the ocean, as well as in the atmosphere, observations are much more closely spaced in the vertical than in the horizontal. This is needed because the scales of ocean variability are much shorter in the vertical than in the horizontal. Thus, the vertical coordinates must be expanded in such a way that the distances $(X\text{-}X_i)$ in Equation III.4 are effectively nondimensionalized by horizontal and vertical length scales appropriate for the data being analyzed. The proper amount of vertical coordinates expansion must be determined and here again we are forced to use a trial and error process, although the aspect ratios in common practice in oceanography provide a guideline. The best results were found using an aspect ratio of approximately 1/2100 corresponding to normalizing the horizontal coordinates (dividing by the length of the shortest grid domain axis) and leaving the vertical

coordinates unchanged. Scaling the vertical dimension by dividing by the maximum depth (aspect ratio of approximately 1/44) yielded very poor results, but there should be several possible combinations of the smoothing parameter, interpolation constant, mean-square errors and aspect ratio that can give reasonably good results. For a more complete discussion of the sensitivity of the method, and procedures to help specify the scaling and smoothing parameters, the reader is referred to Nuss and Titley (1993).

The multiquadric interpolation method outlined above was applied to the CTD stations after the processing described in the previous section and after appending four new "stations" with SAIL data to the vector of observations (see Figure 9). SAIL points were selected with a spacing similar to the CTD stations spacing, and they contain information on temperature and salinity only at the surface. The main purpose of including these four SAIL stations was to determine to what extent the lack of observations directly below surface observations influences the interpolated fields at depth (in this way simulating the future inclusion of satellite data in the interpolation). A minor draw back is that the inclusion of the SAIL data points increases the asynopticity problem, since they were measured on the 21st of May, whereas the CTD casts were collected between the 22nd and the 25th of May.

The multiquadric interpolation was applied in both two and three dimensions separately, with the purpose of comparing the surface temperature analysis produced by the three dimensional version with the analysis using the two dimensional version. The latter uses only the surface temperature values from CTD and SAIL on a 48x45 grid; the grid spacing is 1825 m in the x direction and 1831 m in the y direction. A rotation in the grid domain was applied so the x axis is approximately parallel to the station line with the greater number of stations running roughly in the NW-SE direction (see Figure 9). The coordinate system used is the Universal Transverse Mercator (UTM) with origin of coordinates in the lower left corner of the grid domain (see the U. S. Geological Survey Professional Paper #1395, 1987, for transformation formulae). The limits of the domain were arbitrarily set in order to include the eddy and the cold water in the upper left corner

but to exclude the warm filament to the south (see Figure 4). Some CTD and SAIL stations were intentionally excluded from the domain, also. These data points were included in the computation of the weights and helped fill in the areas without data.

The three dimensional version interpolates grid points in the same horizontal layout as in the two dimensional application, but extending in the vertical down to -2001m. The same preselected levels introduced in section III.B.1 were used here for observation points. The domain was then organized in a long vector of observations to compute the weights and perform the interpolation. The interpolated levels coincide with the observation levels, but this is not necessary in general. Several runs using different interpolation parameters and mean-square errors for the observations were performed, to make a rough estimate of the optimal parameters. The results of the two and three dimensional versions were then visualized using the Explorer visualization package.

The results obtained with the multiquadric interpolation of the CTD and SAIL data are presented and discussed in the next chapter.

IV. RESULTS

This chapter presents the results obtained with multiquadric interpolation of the raw CTD and SAIL data into the grid domain starting with the two dimensional case, which is then compared to the surface map generated from the three dimensional multiquadric results.

A. TWO DIMENSIONAL MULTIQUADRIC INTERPOLATION

The two dimensional multiquadric interpolation results are presented in Figure 10. These results were obtained by applying a two dimensional version of Equation III.9 to the four SAIL data points and to the average of the first five meters of each CTD station (first three levels), interpolating onto the grid described in the previous section. We are able to identify the major features of the temperature distribution at the surface seen in the two dimensional results by comparing with Figure 4. These features include the regions of warm water on the right side of the domain and at the lower left corner, as well as the cooler water in the upper part of the image. The method was also able to reproduce the general regions of cold and warm water in the interior of the domain that can be seen in the satellite image. Of course, an exact match of the interpolated results with the satellite image is not possible to achieve, in the first place because the satellite image is a high resolution snapshot of the surface temperature field at an instant in time near the beginning of the cruise, and in the second place because of the temporal bias between the remotely observed temperatures and the CTD observations, discussed in section III.A.

The influence of the lack of synopticity between the satellite derived temperatures and the CTD and SAIL observations on the analysis can now be further quantified, with the aid of Figures 3, 4, 5 and 10. The low resolution of the CTD and SAIL sampling introduces a high degree of uncertainty in the identification and correspondence between these figures

of mesoscale features, such as the center of the eddy or other features in the outer limits of the eddy.

The determination of the exact location of the center of the eddy on each of the Figures 3, 4 and 10 gives an idea of the translation of the eddy in the horizontal, since these figures present data collected at different instants in time. The interpretation of features other than estimation of the location of the center of the eddy is difficult because there are several mechanisms that can contribute to a temporal change in the shape of the temperature field associated with the eddy (e.g., secondary circulation, horizontal advection, spinning). Furthermore, a positive identification of the existence of an eddy is somewhat uncertain. However, the location of the center of the eddy can be estimated with some precision from the satellite images in Figures 3 and 4 and the multiquadric interpolation results in Figure 10. An analysis of Figure 5 shows that the center was located approximately at 124.3° W and 38.7° N during the one-week period of data collection. This result is supported by the satellite images, in particular Figure 4 that shows a spot of warm water in that same position, just to the northwest of station number 18. In the UTM grid, this station is positioned on grid lines x=34 and y=17, so the pocket of warm water northwest of the station is positioned approximately at grid points x=29 and y=16. Figure 10 shows a warm spot at this position and it is reasonable to assume that it represents the center of the eddy. The existence of a warm region at x=42, y=22 is the result of the strong influence of the relatively warm SAIL stations on the interpolation scheme, causing the generation of a local maximum in this area.

From these combined analysis and observations, it appears that the eddy did not experience significant horizontal translation during the duration of the cruise. Therefore, although there is a time lag between satellite data and hydrographic data as shown in Figure 2, it appears that the effects of time delay on the interpolation procedure are not significant because the eddy remained in approximately the same position. Figures 3 and 4 also show the eddy in the same position over a period of 24 hours, supporting this conclusion. Had the

eddy moved either alongshore or offshore, the discrepancies between the different data sets would be larger, and the level of uncertainty would be increased considerably.

Nothing has been deduced about the rotational aspect of the eddy dynamics, because this is more difficult to detect from the available data. There is no evidence that the warm filament visible in Figure 4 that is located near station number 24 was sampled by this CTD cast (cf. Figure 8). This fact may have several interpretations. One might conclude that the feature moved due to rotation of the eddy. However, this may also be explained by secondary circulations or temporal changes in the field.

The range of values in the grid domain is exactly the same as the surface temperature range observed in the CTD casts. However, the interpolated maximum and minimum temperatures do not occur at the same locations as the observed maximum and minimum temperatures because multiquadric interpolation, by definition, does not fit exactly with the observation points due to a non-zero interpolation constant and numerical truncations.

With these considerations in mind, the method succeeds in keeping the interpolated values within realistic bounds and reproducing in fine detail the surface temperature structure.

B. THREE DIMENSIONAL MULTIQUADRIC INTERPOLATION

A more complete three dimensional multiquadric interpolation algorithm was used to interpolate the CTD observations onto the same horizontal grid domain and along the vertical down to -2001 m. Where necessary, CTD stations were extended as described in section III.B.1. Surface SAIL data points were also included in the input to the interpolation. The same levels mentioned in section III.B.1 were used for vertical resolution of the interpolated field.

A series of three dimensional interpolations were performed in a trial and error process in order to roughly estimate the best set of interpolation parameters, the smoothing parameter λ, the interpolation constant c and the uncertainty level σ, from Equation III.9. The initial values of these parameters were taken after Nuss (1993). For the purpose of a

first level sensitivity study, several combinations of parameter values were used. Table 2 lists the values used in this work.

TABLE 2: INTERPOLATION CONSTANTS

CONSTANT	*VALUES USED*
λ	0.025 and 0.01
c	0.005, 0.05 and 0.01
σ	0.1, 0.25 and 0.5

A total of six combinations were used, comparing results with the observed CTD temperature values at the first three levels, at the last level and at the level of maximum temperature (this level is z=-3 m for CTD observations, and varied between z=-3 m and z=-15 m for interpolated values). The best set of parameters thus obtained was λ=0.025, σ=0.25 and c=0.005. The three dimensional multiquadric interpolation results for this set of values are presented in Figures 11 through 13.

Figure 11 shows the surface temperature map. Notice the close similarity between this surface map and the one in Figure 10, obtained using only the observed temperature values at the surface. The surface map obtained using the three dimensional algorithm does a very good job in maintaining the interpolated values in the same range and keeping the positions of the main features of warm and cold water, including the assumed center of the eddy. Figure 12 shows several isothermal contours and the isothermal surface of 8 °C. The primary purpose of this figure is to illustrate two results of the three dimensional interpolation: the resulting smooth isothermal surface and the close agreement of this surface with the same surface produced by the analysis of raw CTD data (Figure 6), showing that with the chosen set of parameters the method produces good results both in the horizontal and in the vertical.

The three dimensional results, as far as smoothing is concerned, can be affected not only by the smoothing parameter λ and uncertainty level σ, but also by the vertical

distribution of observation points. As mentioned previously, the vertical levels of observed points were selected to give more resolution in the upper ocean and less resolution as depth increases. It was noticed that this fact is probably the cause of the appearance of small scale noise in the interpolated deeper levels, mostly below z=-1000 m. This is evident in Figure 13. The main feature of this figure is the isothermal surface of 3 °C with small amplitude, small scale ripples. These ripples are artificially introduced by the interpolation algorithm. A possible way to reduce this noise is by setting the σ parameter as a vertically varying parameter, keeping the level of smoothing in the upper levels and increasing the smoothing in the lower levels. Another possibility to reduce the noise is to make a thorough parameter sensitivity study, using reference criteria other than the one mentioned above, or extending that criterion to include the resulting variability in the deeper levels. This way, a different optimal set of parameters could be selected. Both approaches will be taken in future work.

V. CONCLUSIONS AND RECOMENDATIONS

Hydrographic and satellite-derived data were analyzed and processed to evaluate them for possible input in a coastal circulation model. The hydrographic data consisted of a set of 32 CTD casts yielding salinity, temperature and pressure every 2 m in the vertical from the surface and four additional points with salinity and temperature data only at the surface. This data was collected between 21 and 25 May off Point Arena, California. Satellite data was obtained from channel four of the AVHRR for day 22 May.

The hydrographic data was used in a first analysis to verify the information contained in the satellite image (Figure 4) using three dimensional visualization (section III.B.1). This image shows an eddy of cold water with some warm water possibly entrained from its outer edge. The hydrographic data verified the existence of the eddy, and revealed its manifestation in the vertical, but showed no clear evidence of the origin of the warm water entrainment, possibly due to the low resolution of the data.

The satellite data was then processed for future use. Since this data is affected by atmospheric effects and by a time bias relative to the CTD stations, an adjustment was performed to reduce the difference between the satellite temperatures and the CTD surface temperatures in a optimal way (section III.A).

The hydrographic data was then interpolated from the observations domain into a grid domain that can eventually be used in a coastal circulation model (section III.B.2). To interpolate the data the method of multiquadric interpolation was used. This method was applied in both two dimensional and three dimensional versions, to compare the surface results one against the other and against the satellite image. Several runs to make a rough estimate of the method's optimal parameters in the three dimensional case were performed (section IV.B). The results obtained are described in chapter IV, with pertinent figures contained in the appendix.

Based on the research outlined above, the following conclusions are made:

- The hydrographic data verify the satellite observations, demonstrating that the satellite image indeed depicts an oceanic eddy, and not, for example, an atmospheric eddy. A particular feature of the eddy, the warm pocket of water visible in the satellite image, was also sampled by the CTD casts;
- This eddy has a vertical signature down to approximately z=-300 m;
- During the period covered by the cruise the eddy did not undergo any visible translation movement thus making the lack of synopticity between the satellite-derived and in situ hydrographic data not significant for the purpose of objective analysis;
- The method of multiquadric interpolation does a very good job in extending the observed temperature field outside the spatial domain defined by the hydrographic data, both in the horizontal and in the vertical;
- The sensitivity of the multiquadric interpolation to the interpolation constants and to the resolution of the observed data is an important factor, particularly in the smoothing of the interpolated field.

During this research some aspects of the data interpolation method suggest work to be done in the future:

- Parameter sensitivity study. This will allow a more accurate determination of the optimal parameters;
- Reduction of small scale noise in the deeper levels of the interpolated temperature field;
- Static stability analysis. The combination of temperature and salinity observations to compute the stability of the entire grid domain, thus providing a better reference for the performance of the multiquadric interpolation;
- Inclusion of satellite-derived surface temperatures in the observations vector, to improve the description of the temperature field not only in the horizontal but also, by means of the multiquadric analysis, in the underlying column of water.

LIST OF REFERENCES

Acoustic Doppler Current Profilers, *Principles of Operation: A Practical Primer*, RD Instruments, 1989.

Batteen, M. L., Rutherford, M. J. and Bayler, E. J., 'A Numerical Study of Wind- and Thermal-Forcing Effects on the Ocean Circulation off Western Australia", *Journal of Physical Oceanography*, V. 22, No. 12, pp. 1406-1433, 1 December 1992.

Explorer, *Iris Explorer User's Guide*,Version 2.0, Silicon Graphics, Inc, Document Number 007-1371-010, 1993.

Gill, A. E., *Atmosphere-Ocean Dynamics*, pp. 425-428, Academic Press, Inc., 1982.

Haltiner, G. J., and Williams, R. T., *Numerical Prediction and Dynamic Meteorology*, 2d ed., pp. 356-385, John Wiley & Sons, Inc., 1980.

Hardy, R. L., "Multiquadric Equations for Topography and Other Irregular Surfaces", *Journal of Geophysical Research*, V. 76, pp. 1905-1915, 1971.

Haynes, R. and Barton, E. D., "Lagrangian Observations in the Iberian Coastal Transition Zone", *Journal of Geophysical Research*, V. 96, No. C8, pp. 14731-14741, 15 August 1991.

Linpack, Argonne National Laboratories, University of New Mexico, 1978.

Matlab, *Matlab User's Guide*, Version 4.0, The Mathworks, 1992.

Nuss, W. A., and Titley, D. W., "Use of Multiquadric Interpolation for Meteorological Objective Analysis", paper submitted to *Monthly Weather Review*, May 1993.

Nuss, W. A., "Three Dimensional Meteorological Analysis Using Multiquadric Interpolation", 1993, unpublished.

Pares-Sierra, A., White, W. B. and Tai, C.-K., "Wind-Driven Coastal Generation of Annual Mesoscale Activity in the California Current", *Journal of Physical Oceanography*, V. 23, No. 6, pp. 1110-1121, 1 June 1993.

Ramp, S. R., Jessen, P. F., Brink, K. H., Niiler, P. P., Dagget, F. L. and Best, J. S., "The Physical Structure of Cold Filaments Near Point Arena, California, During June 1987", *Journal of Geophysical Research*, V. 96, No. C8, pp. 14859-14883, 15 August 1991.

Sousa, F. M. and Bricaud, A., "Satellite-Derived Phytoplankton Pigment Structure in the Portuguese Upwelling Area", *Journal of Geophysical Research*, V. 97, No. C7, pp. 11343-11356, 15 July 1992.

Strub, P. T., Kosro, P. M. and Huyer, A., "The Nature of the Cold Filaments in the California Current System", *Journal of Geophysical Research*, V. 96, No. C8, pp. 14743-14768, 15 August 1991.

U. S. Geological Survey Professional Paper #1395, *Map Projections - A Working Manual*, by John P. Snyder,p. 58, 1987.

APPENDIX - FIGURES

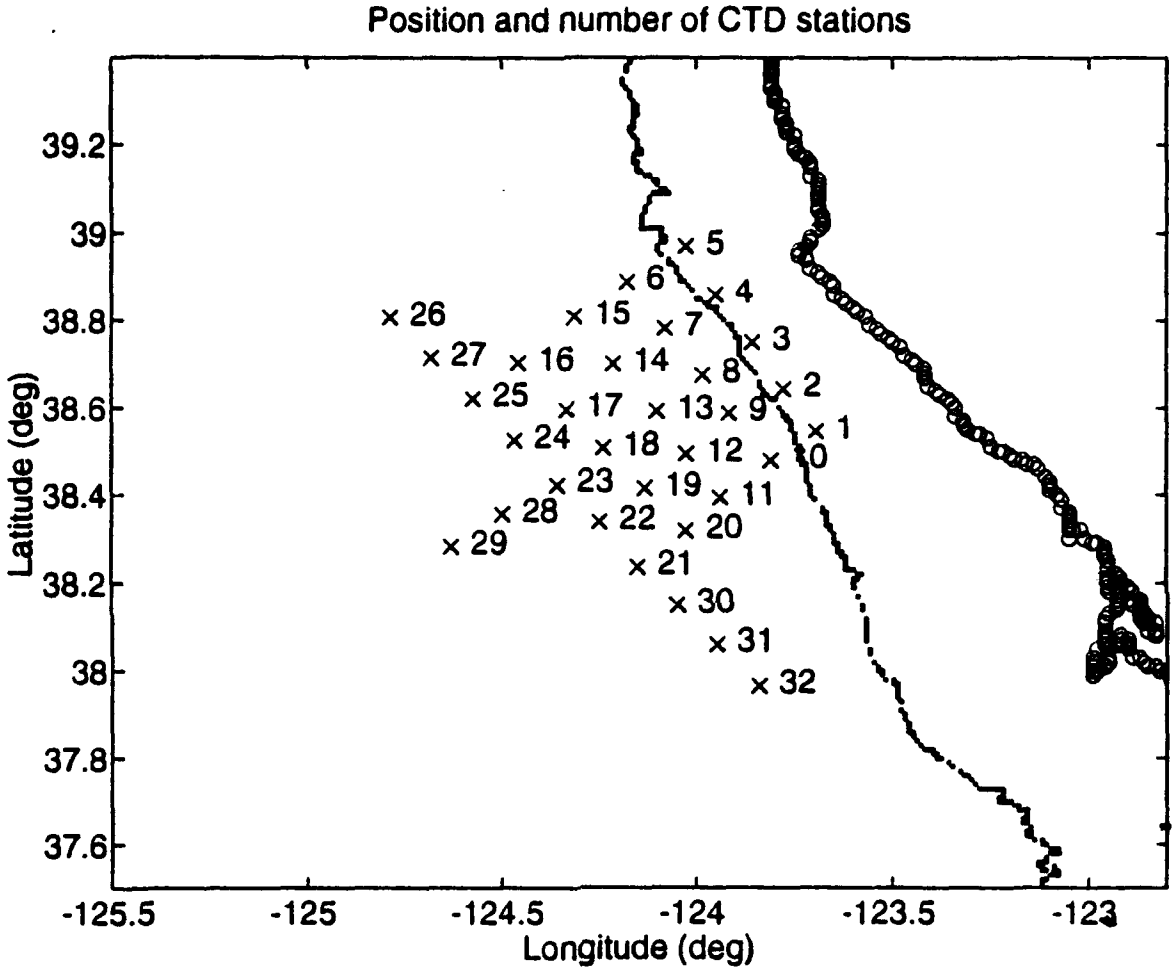

Figure 1 - Position and number of CTD stations.

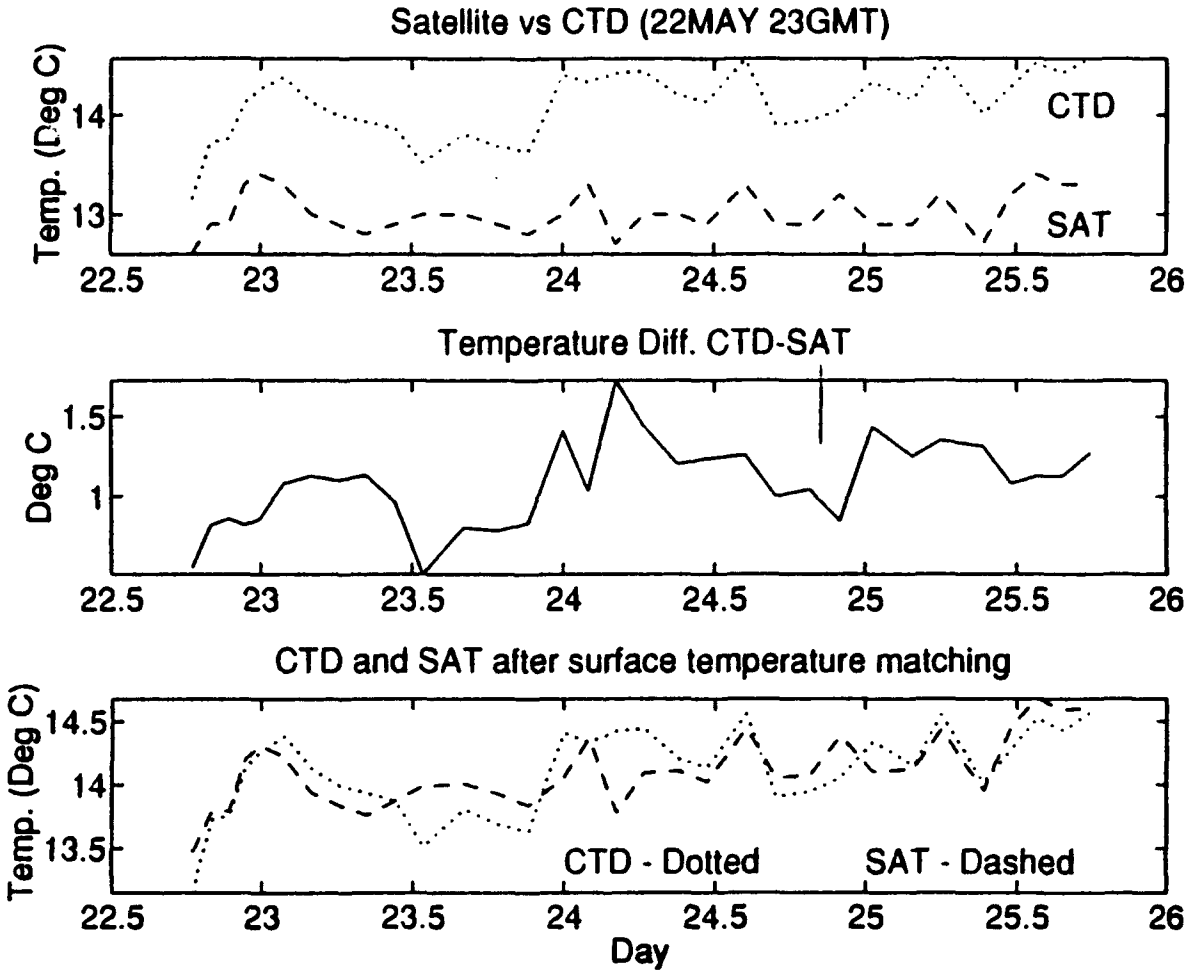

Figure 2 - Analysis of Sea Surface Temperature (SST). Top figure: comparison of CTD and satellite derived SST (SAT); middle figure: difference between the two SST series; bottom figure: comparison of CTD and adjusted satellite derived SST.

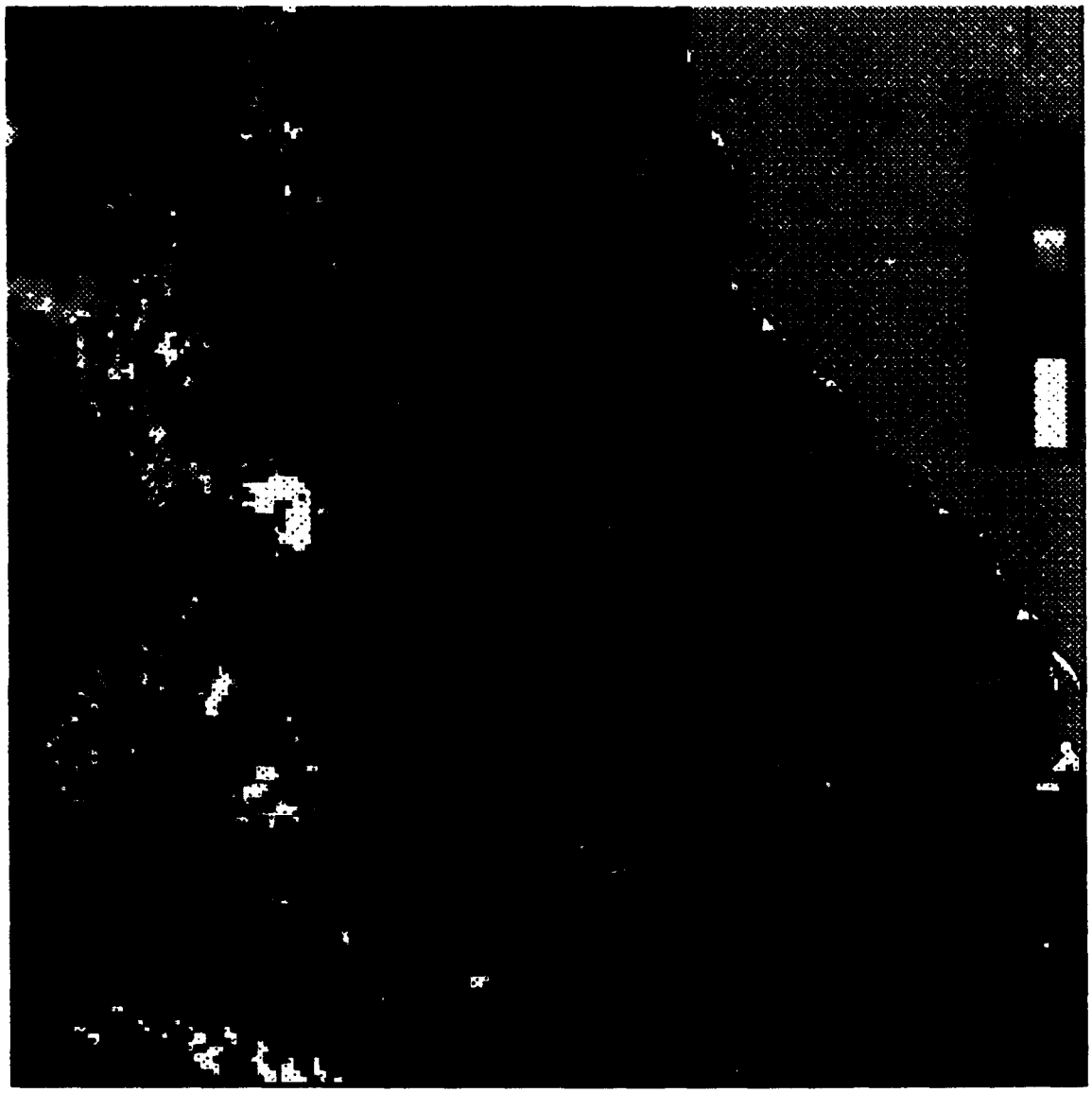

Figure 3 - National Oceanic and Atmospheric Administration (NOAA) satellite image, obtained from Channel 4 of the Advanced Very High Resolution Radiometer (AVHRR), of the Sea Surface Temperature (SST) off Point Arena, on 21 May 1993, 23 GMT. The crosses represent the positions of the CTD stations (temperatures in degrees Celsius).

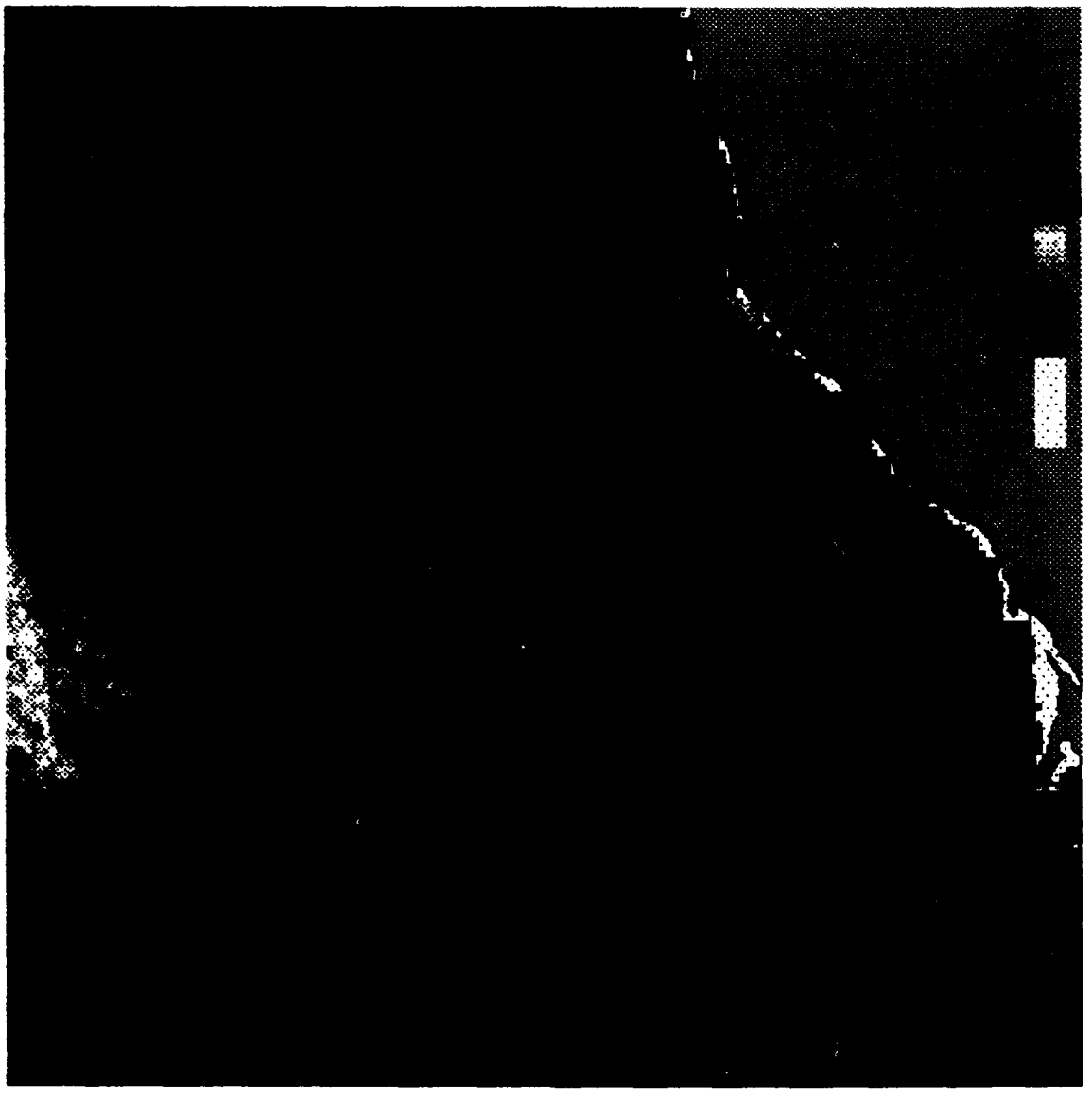

Figure 4 - National Oceanic and Atmospheric Administration (NOAA) satellite image, obtained from Channel 4 of the Advanced Very High Resolution Radiometer (AVHRR), of the Sea Surface Temperature (SST) off Point Arena, on 22 May 1993, 23 GMT. The crosses represent the positions of the CTD stations (temperatures in degrees Celsius).

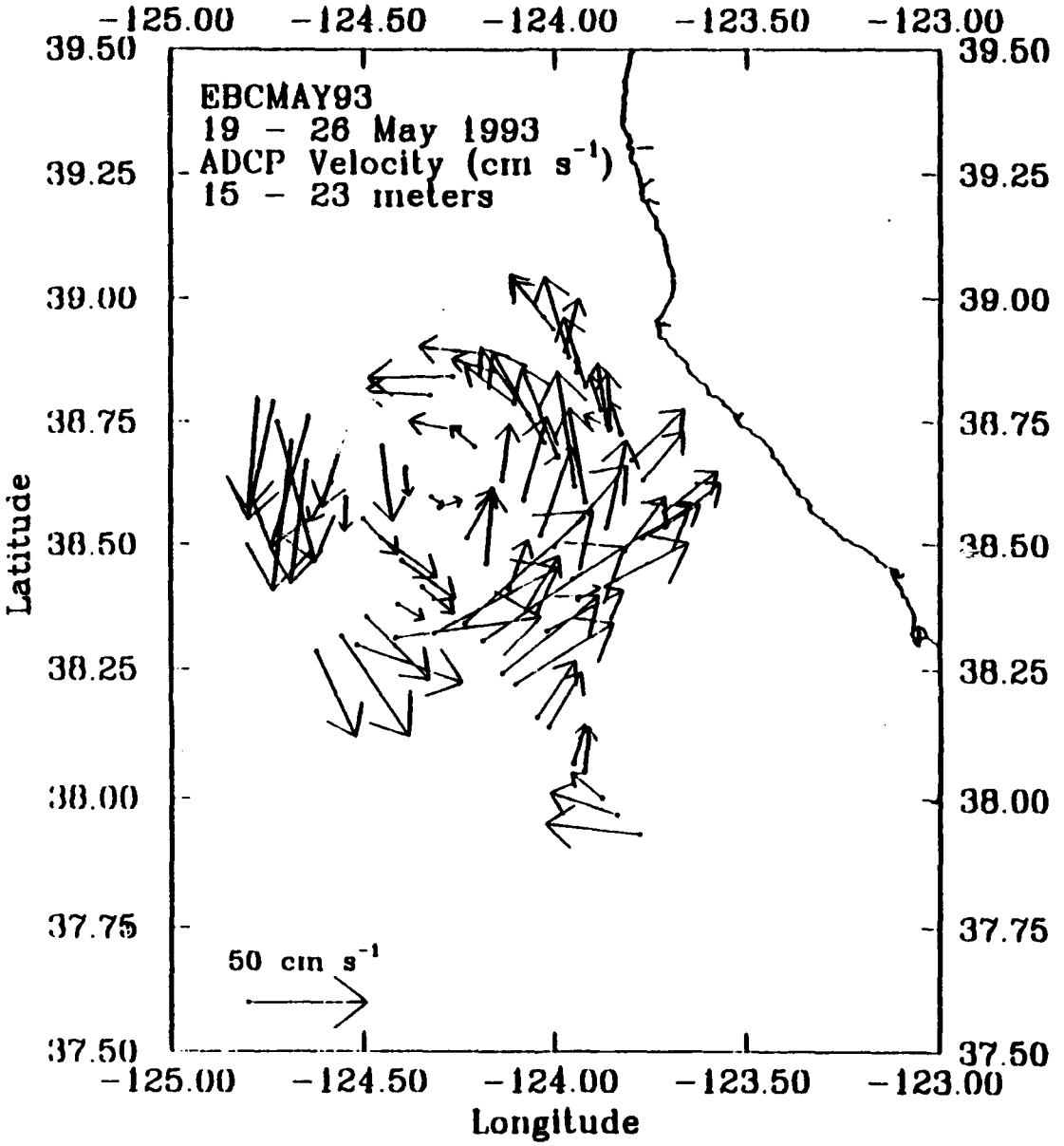

Figure 5 - Acoustic Doppler Current Profiler (ADCP) instantaneous horizontal velocity vectors for depth bin 15-23 meters, for the period 19 to 26 May 1993.

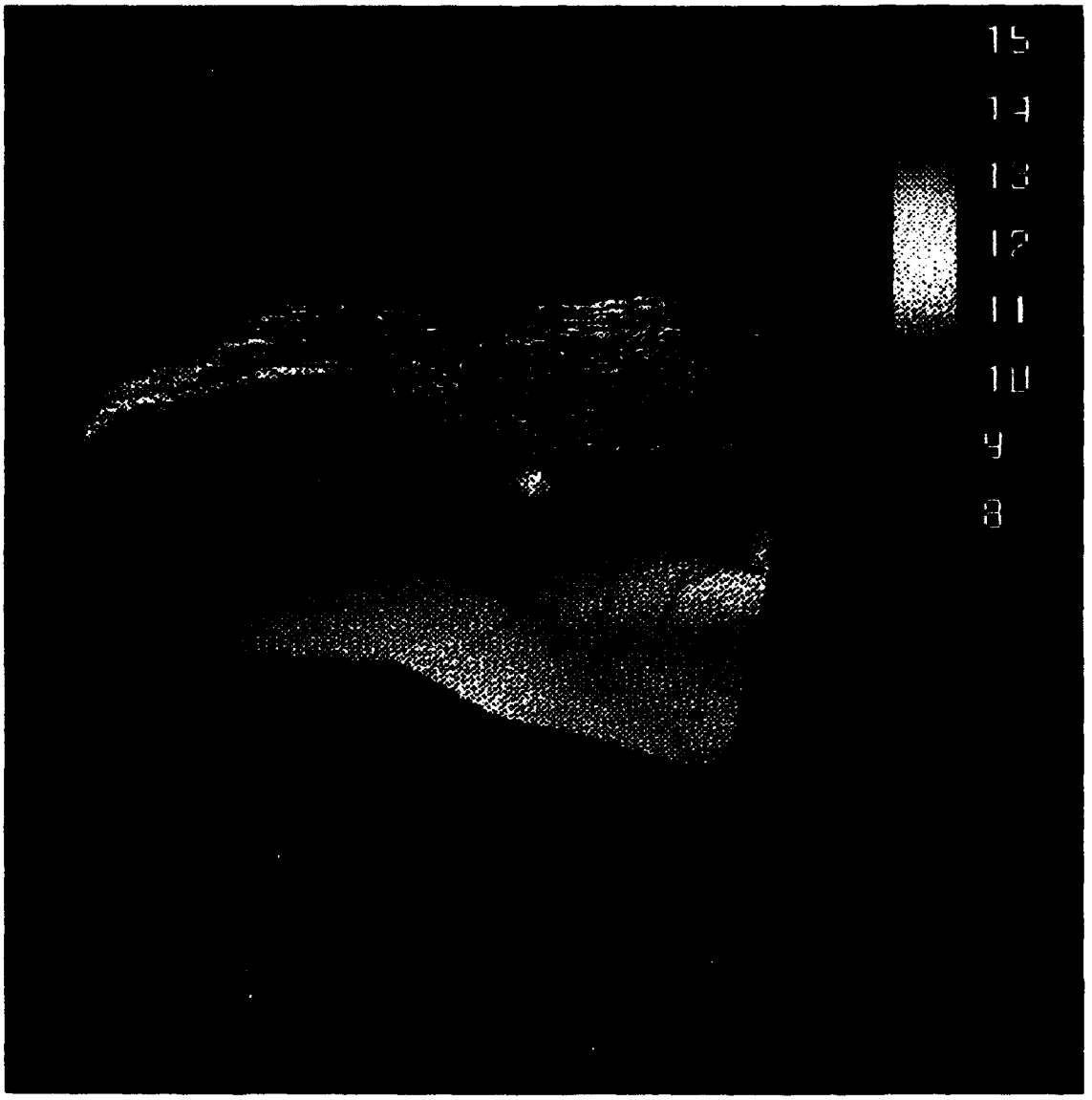

Figure 6 - Three dimensional visualization of raw CTD data on a 5x5 station grid. The figure shows an isothermal surface (8 °C), several isothermal contours and a vertical section of temperature along CTD stations number 5, 6, 15, 16 and 25 (temperatures in degrees Celsius).

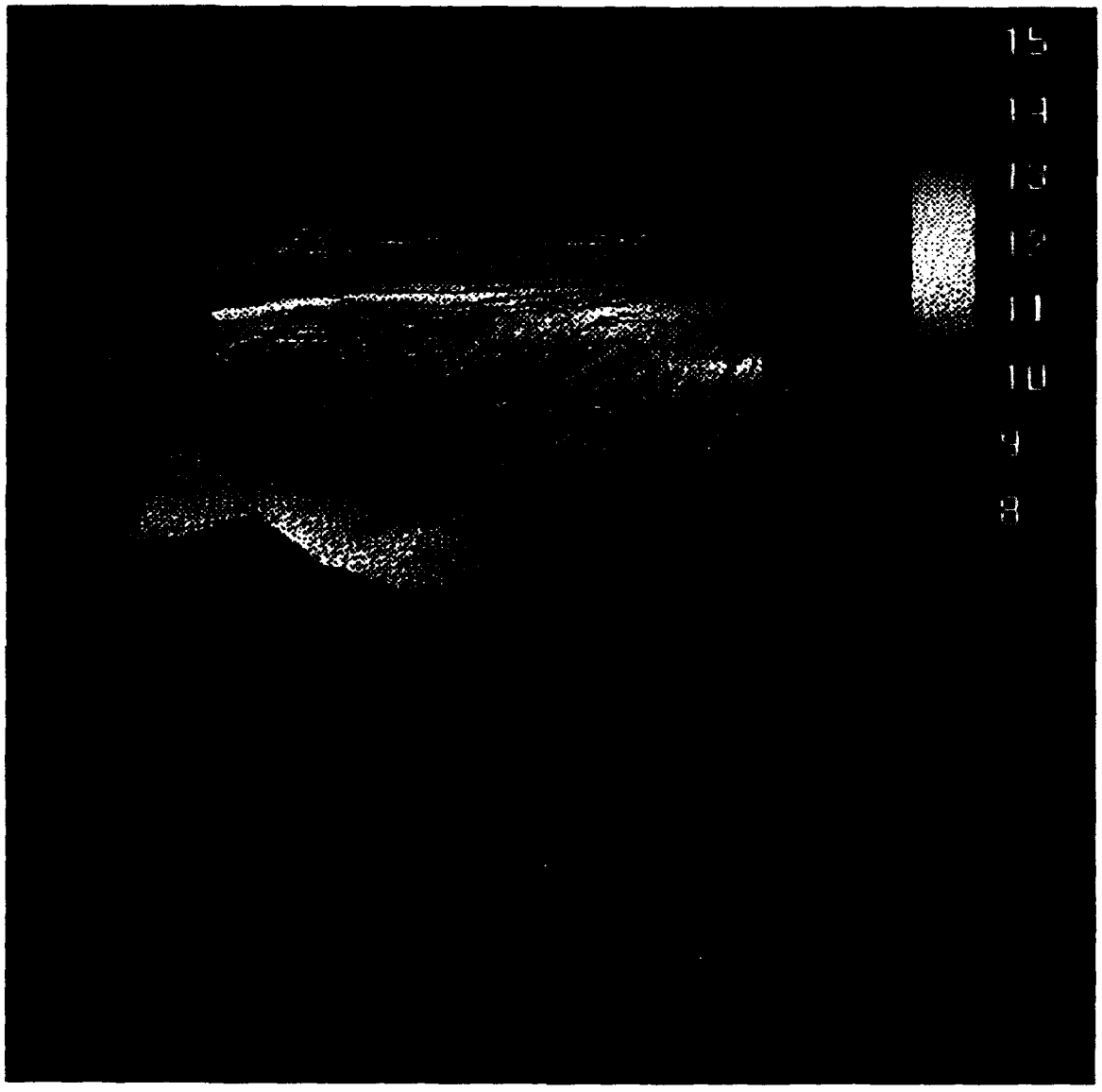

Figure 7 - Three dimensional visualization of raw CTD data on a 5x5 station grid. The figure shows an isothermal surface (8.5 °C), several isothermal contours and a vertical section of temperature along CTD stations number 15, 14, 13, 12 and 11 (temperatures in degrees Celsius).

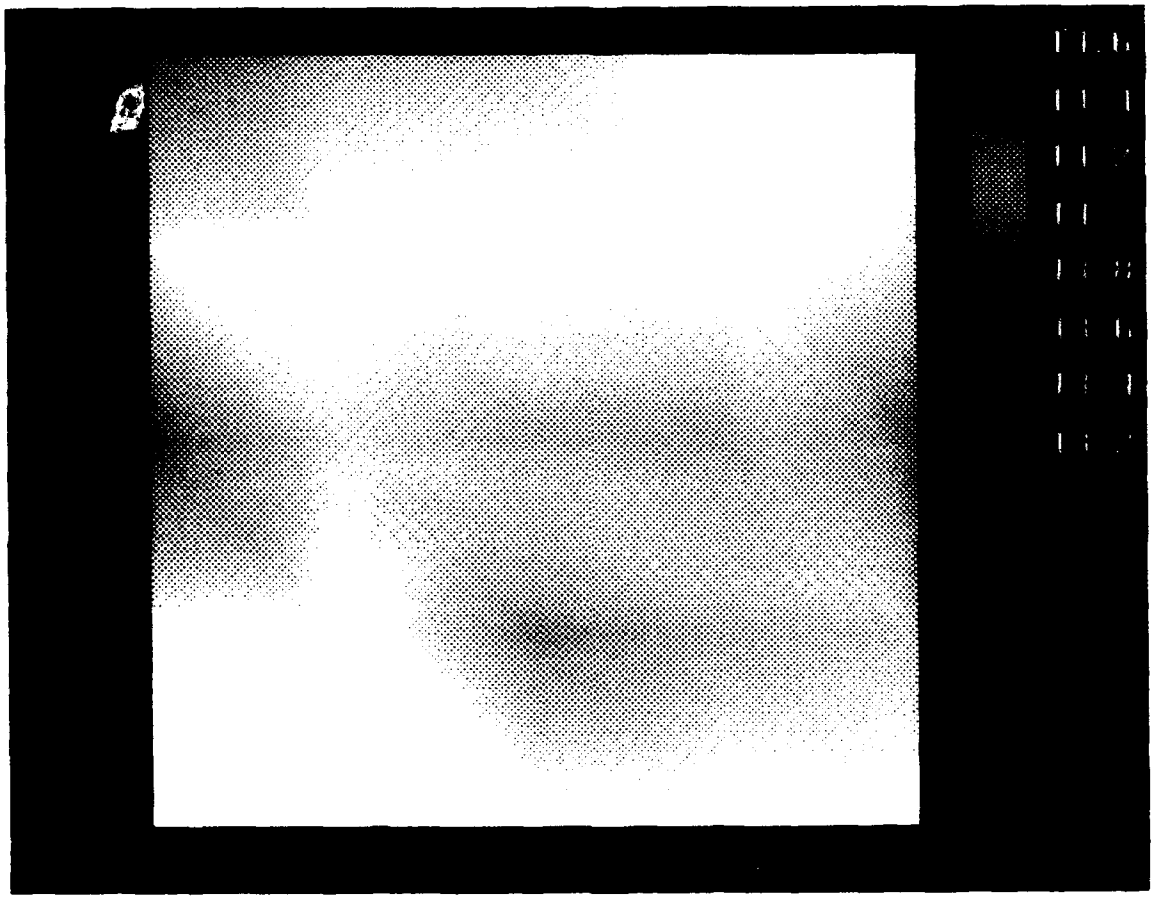

Figure 8 - Two dimensional visualization of Sea Surface Temperatures (SST) on a 5x5 station grid. The figure was obtained by averaging the first 5 m of raw CTD data (temperatures in degrees Celsius). The lower left corner corresponds to station number 25.

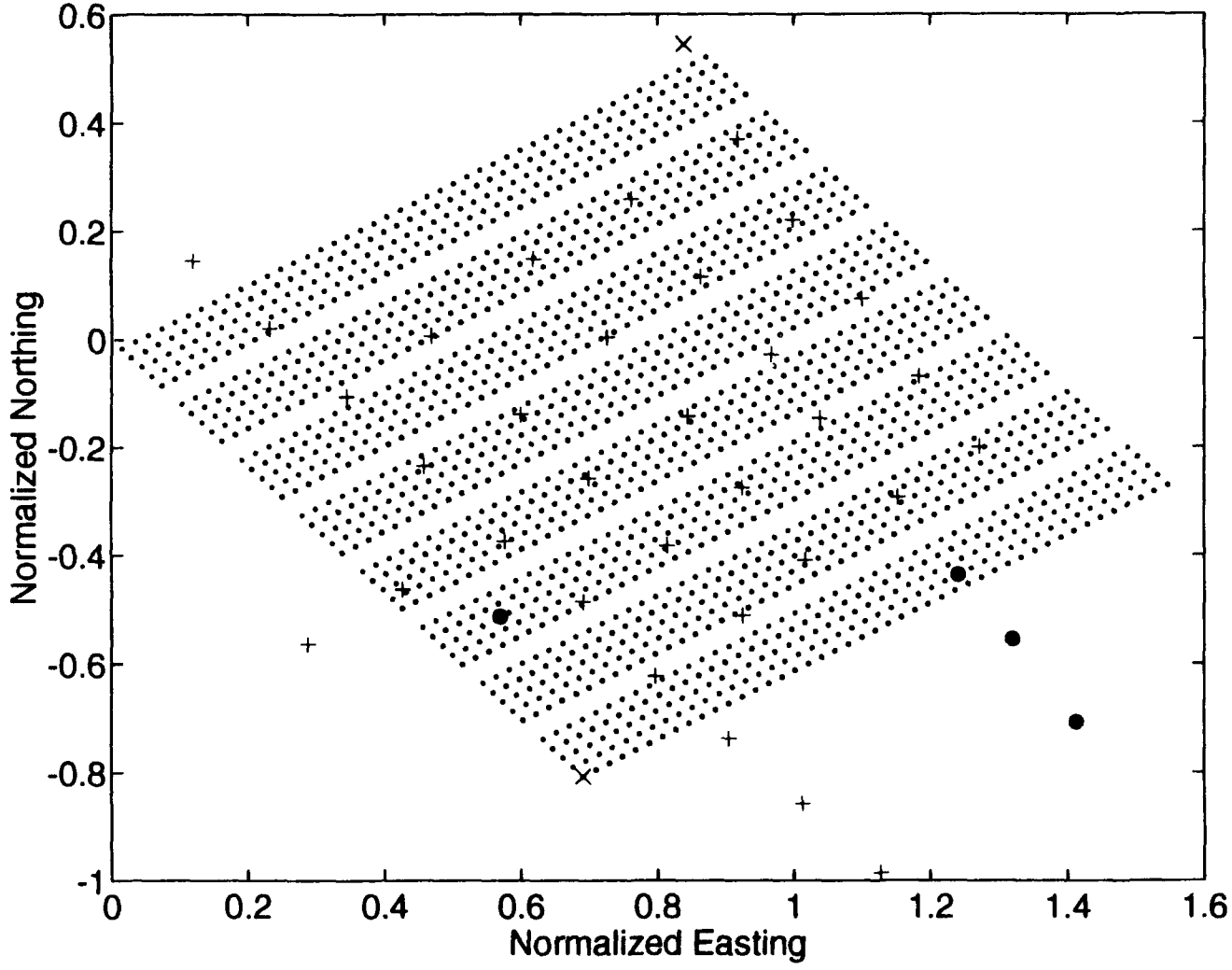

Figure 9 - Grid layout used in the multiquadric interpolation, in UTM coordinates. The X-marks are control points that define the grid domain. The crosses represent the positions of the CTD stations. The circles represent the positions of the SAIL stations. The origin of the grid (point 0-0) corresponds to geographical position 38.7 ° N, 124.9 ° W. The grid is dimensionless.

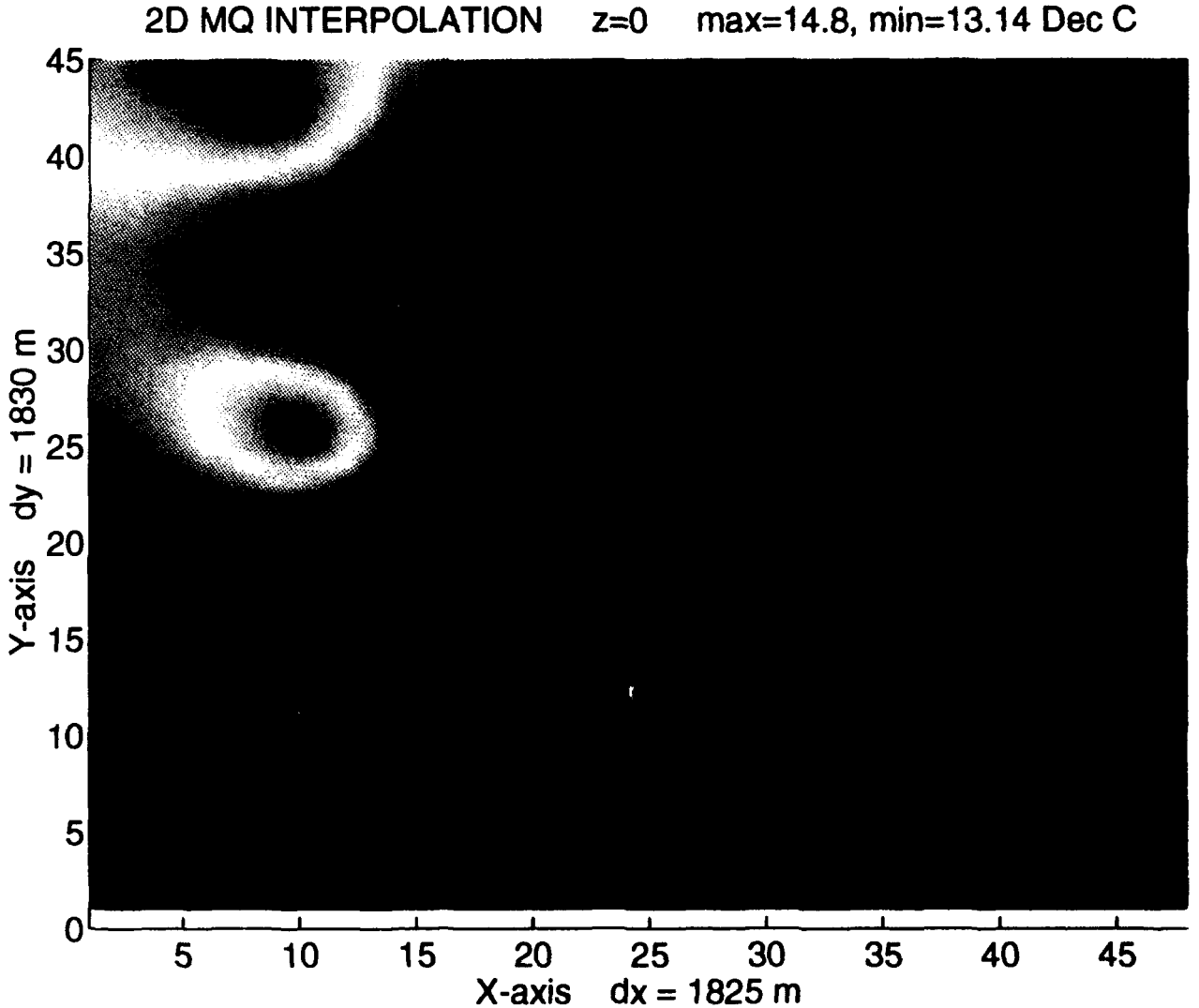

Figure 10 - Map of SST obtained with the two dimensional version of multiquadric interpolation. The lower left corner corresponds to the origin of the grid. Red coming from green is cold water, red coming from blue is warm water.

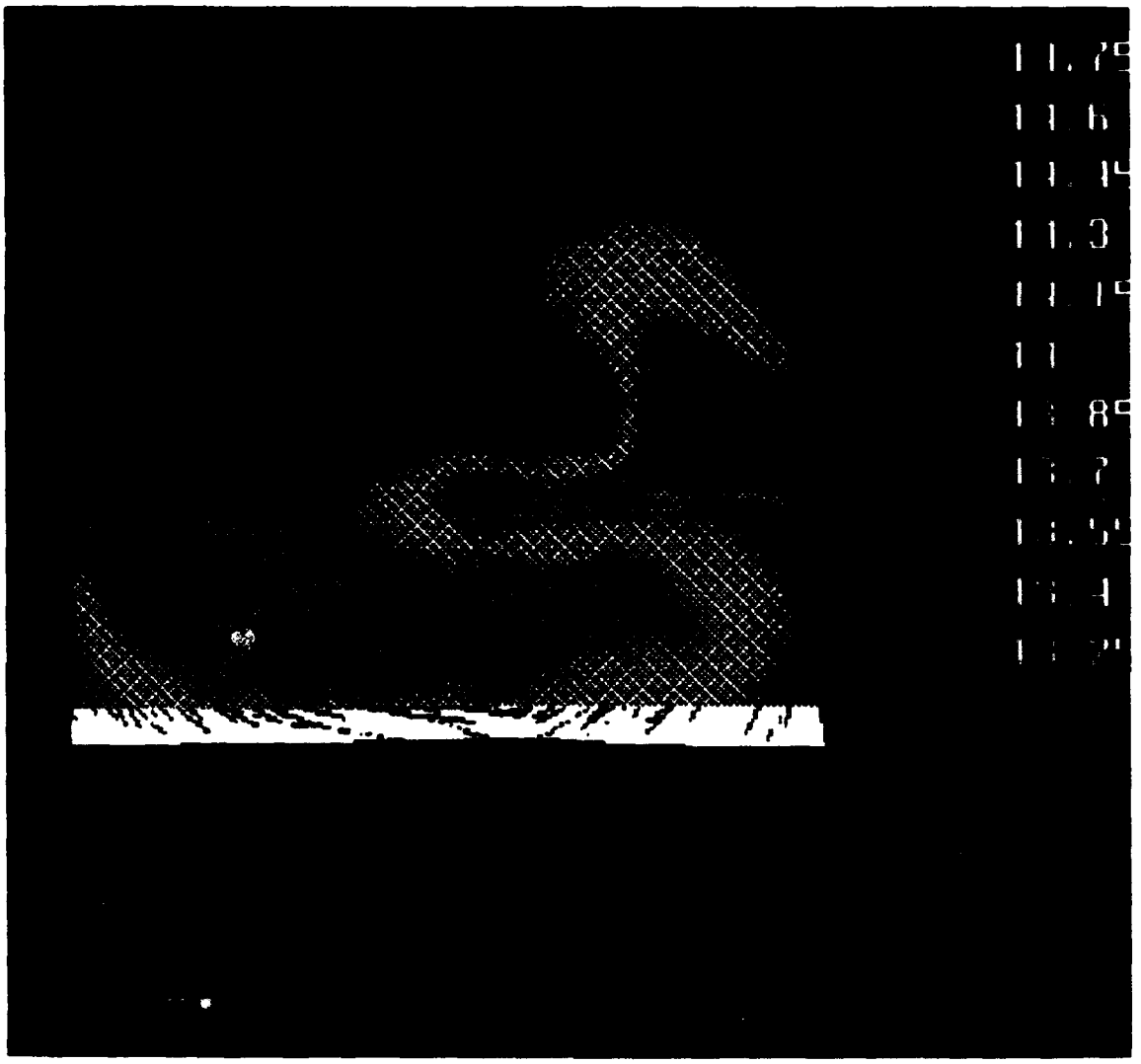

Figure 11 - Map of Sea Surface Temperatures (SST) obtained with the three dimensional version of multiquadric interpolation. The lower left corner of the image corresponds to the origin of the grid. Temperatures in degrees Celsius.

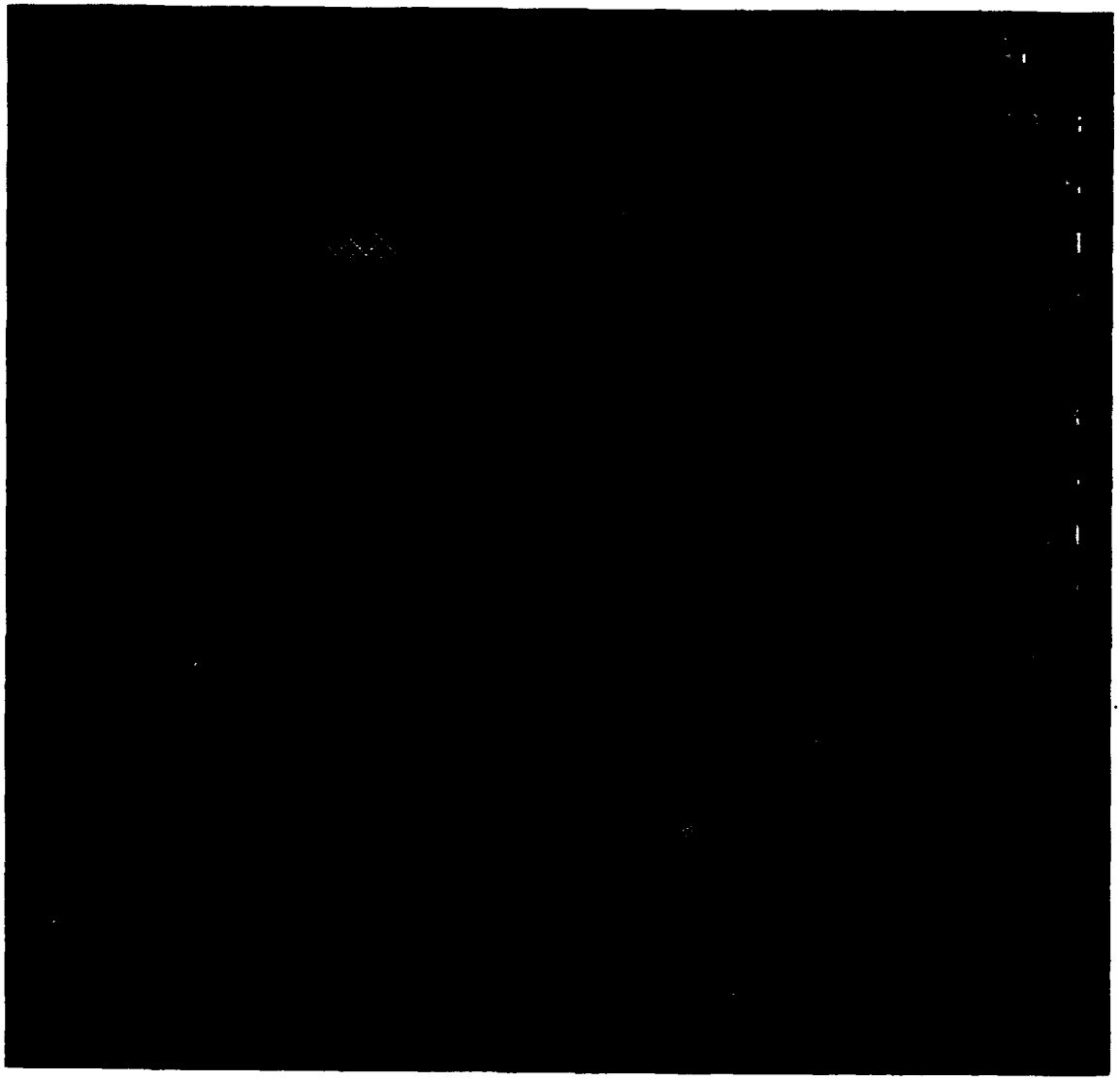

Figure 12 - Three dimensional visualization of interpolated temperatures, obtained from the three dimensional version of multiquadric interpolation. The figure shows a surface temperature map, several isothermal contours and an isothermal surface (8 °C). Temperatures in degrees Celsius.

Figure 13 - Three dimensional visualization of interpolated temperatures, obtained from the three dimensional version of multiquadric interpolation. The figure shows a surface temperature map, several isothermal contours and an isothermal surface (3 °C). Temperatures in degrees Celsius.

INITIAL DISTRIBUTION LIST

Defense Technical Information Center Cameron Station Alexandria, VA 221314	2
Librarian Code 52 Naval Postgraduate School 411 Dyer Rd. Rm 104 Monterey, CA 93943-5101	2
Director of Research Administration Code 012 Naval Postgraduate School Monterey, CA 93943	1
Oceanography Department Code OC/Co Naval Postgraduate School 833 Dyer Rd. Rm 331 Monterey, CA 93943-5122	1
Roland W. Garwood, Jr. Code OC/Gd Naval Postgraduate School 833 Dyer Rd. Rm 308 Monterey, CA 93943	1
Robert L. Haney Code MR/Hy Naval Postgraduate School 589 Dyer Rd. Rm 252 Monterey, CA 93943-5114	1
Dr. Steve Ramp Office of Naval Research Code 322PO 800 N. Quincy St. Arlington, VA 22217	1

Dr. Manuel Fiadeiro
Office of Naval Research
Code 322PO
800 N. Quincy St.
Arlington, VA 22217

1

Direcção do Serviço de Instrução e Treino
Marinha Portuguesa
Rua do Arsenal
1100 Lisboa
Portugal

1

Director-Geral do Instituto Hidrográfico
Instituto Hidrográfico
Rua das Trinas, 49
1200 Lisboa
Portugal

2

LT Rogério P. Chumbinho
Department of Oceanography
833 Dyer Rd. Rm 312
Naval Postgraduate School
Monterey, CA 93943

1